JOURNAL OF VIROLOGY, May 1992, p. 2990–3002
0022-538X/92/052990-13$02.00/0

Vol. 66, No. 5

Modification of Some Biological Properties of HeLa Cells Containing Adeno-Associated Virus DNA Integrated into Chromosome 17

CHRISTIAN WALZ AND JÖRG R. SCHLEHOFER*

Angewandte Tumorvirologie, Deutsches Krebsforschungszentrum, Im Neuenheimer Feld 506, D-6900 Heidelberg, Germany

Received 5 August 1991/Accepted 16 February 1992

Parvoviruses are known to interfere with cellular transformation and carcinogenesis. Since infecting adeno-associated virus (AAV) frequently integrates its DNA into the cellular genome, we analyzed whether this integration influences the transformed phenotype of the human tumor cell line HeLa. Analysis of three independent HeLa cell clones with integrated AAV DNA (HA-3x, HA-16, and HA-28) revealed the following phenotypic changes of these cells: (i) reduced growth rate, (ii) increased serum requirement, (iii) reduced capacity for colony formation in soft agar, (iv) reduced cloning efficiency on plastic, (v) elevated sensitivity to genotoxic agents (*N*-methyl-*N'*-nitro-*N*-nitrosoguanidine, 7,12-dimethylbenz[*a*]anthracene, human tumor necrosis factor alpha, UV irradiation [256 nm], and heat [42°C]), and (vi) reduced sensitivity to the cytolytic effect of parvovirus H-1. Reduced growth rate and enhanced sensitivity to gamma irradiation were also observed in vivo when tumors from AAV DNA-containing HeLa cells were transplanted into nude mice. This alteration of the biological properties of HeLa cells was independent of the number of AAV genomes integrated, the physical structure of integrated AAV DNA, and the transcription of AAV genes. Integration of AAV DNA was found to occur preferentially on the long arm of chromosome 17 in the three HeLa cell clones analyzed. These findings demonstrate that genomic integration of AAV DNA can alter the biological properties of human tumor cells.

The human helper virus-dependent parvovirus adeno-associated virus (AAV) has been shown to interfere with tumorigenesis at different stages of tumor development (for a review, see references 45 and 46). AAV interferes with adenovirus-induced tumors in hamsters (19, 30, 38) and reduces the growth of hamster tumors derived from cell lines transformed by adenoviruses or herpesviruses (18, 42). AAV can inhibit the transformation of cells induced by adenovirus (11), bovine papillomavirus (27), or the *ras* oncogene (29). Cellular and molecular studies revealed similar effects of AAV on cells in culture: AAV infection was shown to inhibit carcinogen- or virus-induced mutagenicity (53) as well as the selective DNA amplification mediated by these initiating agents (24, 52, 54, 55, 62). In addition, preferential killing of carcinogen-treated cells and of cells derived from malignant human tumors by infection with AAV has been demonstrated (1, 25).

AAVs infect humans without known pathological consequences (5–7, 17, 26). However, AAV may also play a tumor-suppressive role in humans. It appears from seroepidemiological studies that individuals with high antibody titers to AAV are less prone to develop cancer (22, 37, 57). This finding seems to be most significant for cervical cancer.

It has been observed that infection of cultured cells of human origin by AAV frequently results in integration of the viral DNA into the host cell genome (13, 23, 28, 34). Recent reports suggest that the integration occurs preferentially into chromosome 19 of human cell lines (32, 33, 51).

It is not known under what circumstances AAV DNA is integrated into the genome of infected cells in vivo or in which cell types or organs AAV is able to establish a latent infection. In view of the serological studies suggesting a tumor-protective effect (see above), we analyzed whether genomic integration of infecting AAV DNA can modify the properties of the human cervical carcinoma cell line HeLa. This study is also interesting in view of various in vitro systems in which infection of cells with AAV interferes with a variety of events linked to transformation or with tumor development in laboratory animals (see above).

MATERIALS AND METHODS

Cells. HaCaT cells (9), HeLa cells, and HeLa-derived cellular clones were maintained in Dulbecco's modified Eagle's minimal essential medium (DMEM) supplemented with 5% fetal calf serum (FCS) plus antibiotics and grown at 5% CO_2 in a humidified atmosphere.

Virus. AAV type 2 (AAV-2) was prepared from adenovirus type 2- and AAV-2-infected HeLa cells. Cultures showing complete (adenovirus type 2-induced) cytopathic effect (CPE) were treated by three freeze-thaw cycles. Supernatant containing virus was incubated at 56°C for 1 h to inactivate helper virus.

Chemicals. *N*-Methyl-*N'*-nitro-*N*-nitrosoguanidine (MNNG) was purchased from Serva, Heidelberg, Germany. 7,12-Dimethylbenz[*a*]anthracene (DMBA) was obtained from Sigma, Munich, Germany. Both chemicals were dissolved in dimethyl sulfoxide (Merck, Darmstadt, Germany).

Establishment of latently infected cell clones. Semiconfluent HeLa cell monolayers were inoculated with AAV-2 at a multiplicity of infection (MOI) of 10 infectious units per cell (virus was incubated at 56°C for 1 h to inactivate adenovirus; see above). After adsorption for 1 h at 37°C, the medium was replenished and the cells were incubated for 2 days, until they reached confluence. Cells were harvested and split 1:4. After reaching semiconfluence, monolayers were superinfected with AAV-2 as above. Two days after the second

* Corresponding author.

infection, cells were seeded onto 96-well microplates at a concentration of one cell per well. To test for the presence of AAV-2 in the outgrowing cell clones, aliquots of cells were transferred to Gene-Screen filters (dispersed-cell assay [61]) and exposed to denaturing buffer (48). DNA was immobilized by baking the filter at 80°C for 1 h. Screening for positive clones was done by hybridization with [α-^{32}P]dTTP-labeled, cloned AAV-2 DNA (see below).

DNA probes. Cloned wild-type AAV-2 DNA, cloned human papillomavirus type 18 (HPV-18) DNA, and cloned p53 cDNA as well as cloned β-actin DNA were radiolabeled with [α-^{32}P]dTTP by nick translation (44) or with [α-^{32}P]dCTP by the random primer technique (21).

Analysis of DNA. High-molecular-weight cellular DNA was extracted with phenol-chloroform-isoamyl alcohol (48).

Restriction enzyme cleavage was performed as recommended by the supplier. Enzymes were obtained from Boehringer-Mannheim (Mannheim), Biolabs (Schwalbach), Pharmacia (Freiburg), and BRL (Eggenstein-Leopoldshafen) (all in Germany). Digested DNA was analyzed by electrophoresis through 0.7% agarose gels in Tris-borate–EDTA electrophoresis buffer (TBE). DNA was transferred to nylon membranes (Gene-Screen; Du Pont-NEN, Dreieich, Germany) (56). DNA immobilized on nylon membranes was hybridized with radiolabeled [α-^{32}P]TTP (Amersham, Braunschweig, Germany) DNA probes (15). Hybridization was performed in 50 mM NaP_i (pH 7.6)–7% sodium dodecyl sulfate (SDS)–1 mM EDTA at 68°C for 16 h with gentle agitation. Southern blots were autoradiographed after three washing steps at 68°C in 1% SDS–50 mM NaP_i (pH 7.2)–1 mM EDTA for 20 min.

Analysis of RNA. From HeLa cells and the cellular clones HA-3x, HA-16, and HA-28, as well as from clones superinfected with adenovirus and treated with cytotoxic agents (see below), cytoplasmic RNA was prepared by the acid guanidinium thiocyanate-phenol-chloroform extraction technique (15). Polyadenylated [poly(A)$^+$] mRNA was prepared from 5×10^7 cells with the Fast Track mRNA Isolation Kit (Invitrogen, San Diego, Calif.).

RNA was separated by electrophoresis through a 1% agarose gel in morpholinepropanesulfonic acid buffer (MOPS [48]), blotted to nylon membranes (GeneScreen; Du Pont-NEN, Dreieich, Germany), and probed with radiolabeled probes as indicated above.

Preparation of metaphases. Metaphase chromosomes were prepared by the standard air-drying technique. Semiconfluent monolayers were growth-arrested by colcemide (Serva) at a final concentration of 0.1 mg/ml of medium for 1.5 h, treated with a hypotonic KCl solution (0.075 M) for 20 to 30 min, fixed in methanol–acetic acid (3:1, vol/vol) for 30 min with several changes of fixative, and dropped onto slides. Freshly prepared slides were stained after thermal pretreatment at 95°C by the trypsin-Giemsa method (59).

Analysis of chromosomes was done on photographed metaphases. At least 15 spreads were analyzed per cell line, and 50 cells were examined for total chromosome number.

In situ hybridization. Cellular clones containing AAV-2 DNA and HeLa cells (control) were treated with 0.1 mg of colcemide per ml of medium for 2 h prior to fixation. Metaphase spreads on glass slides were made by the conventional Carnoy B fixation method (acetic acid-ethanol-chloroform) after hypotonic treatment with 0.075 M KCl at 37°C for 30 min. The preparations were washed in 70% ethanol at 4°C for at least 24 h, dehydrated in graded ethanol steps (80, 90, and 100%), and air-dried. Prior to denaturation and hybridization, the chromosome spreads were treated

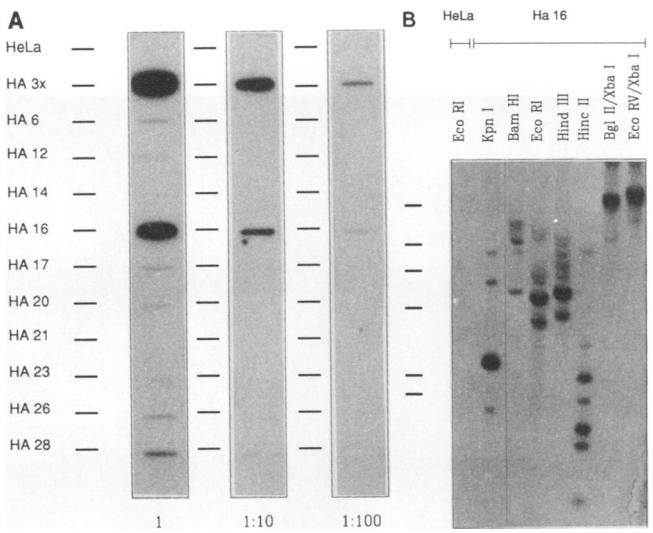

FIG. 1. (A) Slot-blot analysis of persisting AAV-2 DNA in individual cell clones HA-3x, HA-6, HA-12, HA-14, HA-16, HA-17, HA-20, HA-23, HA-26, and HA-28. Cellular DNA (500 ng) was applied to nitrocellulose filters with a slot-blot apparatus. Hybridization with radiolabeled AAV-2 DNA indicates the relative number of integrated virus genomes per cell. The DNA in the slots in the first lane was diluted 1:10 in the second lane and 1:100 in the third lane for quantitation. (B) Southern blot of clone HA-16. High-molecular-weight cellular DNA (10 μg per lane) was cleaved with five different enzymes cutting within the genome of AAV-2 (*Kpn*I, *Bam*HI, *Eco*RI, *Hin*dIII, and *Hin*cII) and three noncutting enzymes (*Bgl*II plus *Xba*I and *Eco*RV plus *Xba*I). DNA was separated by agarose gel electrophoresis, blotted onto a nylon membrane, and hybridized with [α-^{32}P]dTTP-labeled AAV-2 DNA. The analysis shows that AAV-2 DNA is integrated head-to-tail in this cellular clone. Single-cutting enzymes (*Hin*dIII and *Bam*HI) produced a unique fragment of 4.6 kb (as expected), indicating no gross rearrangements of the AAV genomes. Cleavage with noncutting enzymes resulted in large fragments (>23 kb), indicating the integrated state.

with 100 μl of DNase-free RNase (200 μg/ml; Oncor, Gaithersburg, Md.) in 2× SSC (1× SSC is 0.15 M NaCl plus 0.015 M sodium citrate) under a coverslip at 37°C for 1 h. After three consecutive washings in 2× SSC for 5 min each, metaphases were postfixed with 4% formaldehyde in phosphate-buffered saline (PBS)–50 mM $MgCl_2$ for 10 min at room temperature, washed three times for 5 min each with PBS, and dehydrated. Cloned wild-type AAV-2 DNA and cloned p53 cDNA, as well as cloned HPV-18 DNA and "painting" probes (specific for chromosomes 17 and 19), were biotinylated with the BioNick labeling system (BRL Life Technologies, Eggenstein-Leopoldshafen, Germany). Nick translation was performed with biotin-14–dATP in a nick translation mixture (50 μl) containing 1 μg of DNA, 2.5 U of DNA polymerase I, 0.0355 U of DNase I, 0.02 mM dTTP, 0.02 mM dCTP, 0.02 mM dGTP, and standard nick translation buffers. The reaction mixture was incubated at 16°C for 1 h. The reaction was terminated by adding 5 μl of stop buffer (0.1% bromophenol blue, 0.5% dextran blue, 0.1 M NaCl, 20 mM EDTA, 20 mM Tris-HCl [pH 7.8]). Unincorporated nucleotides were separated from the labeled DNA probe by column chromatography with Bio-Gel P-60 (Bio-Rad, Richmond, Calif.) in a 1-ml plastic syringe plugged with siliconized glasswool. The Digoxigenin labeling of AAV-2 DNA was performed by the oligolabeling technique with the Dig-labeling kit from Boehringer, Mannheim, Ger-

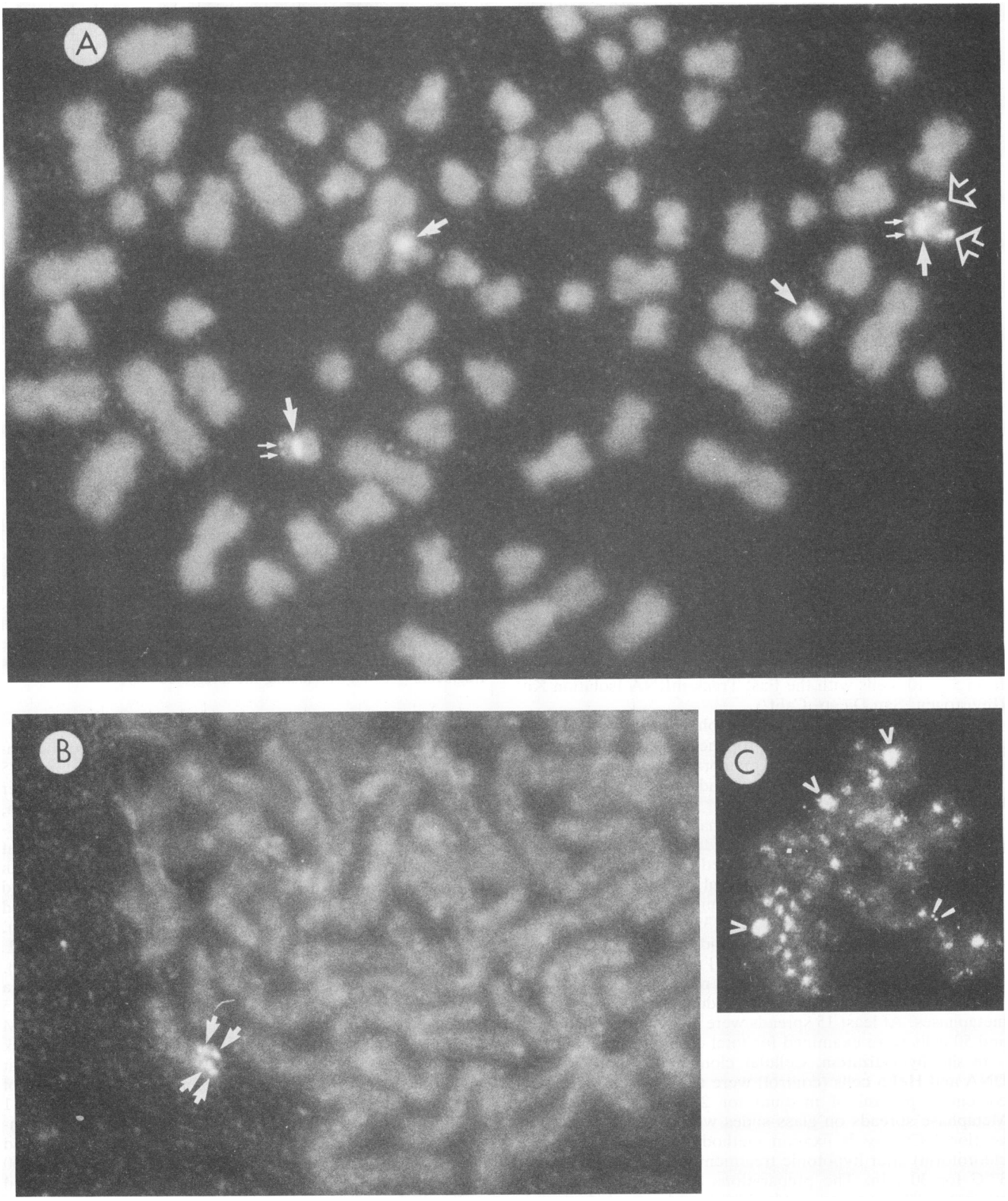
A
B
C

FIG. 2. (A) In situ hybridization with AAV-2 DNA, p53 cDNA, and chromosome 17-specific satellite DNA of a metaphase of clone HA-3x. The large signal within the centromeric region of four chromosomes indicates the chromosome 17-specific centromeric sequences (large single arrows). The small signals at the distal part of the short arms of two chromosomes show the position of the p53 gene (small double arrows). (A p53-specific signal is visible on another chromosome 17 but is out of focus in this photograph; p53-specific signals never lit up on all of the four chromosomes 17 in HeLa cells.) Only one of four chromosomes identified as 17 reveals a signal with AAV DNA, indicating integration at the telomeric region of the long arm (large open arrows). (B) In situ hybridization with the AAV-specific probe and detection with FITC-labeled avidin on a prophase of HA-16 cells. The double signals point towards two integration sites within the telomeric area of the q arm of one chromosome. (C) In situ hybridization of a metaphase of HA-3x cells with the AAV-specific probe labeled with Digoxigenin and simultaneously with a chromosome 19-specific painting probe labeled with biotin. Detection was done with rhodamine-conjugated antibodies and avidin-FITC complex, respectively. Two photographs were superexposed with different emission filters. The low stringency necessary in simultaneous labeling for the painting probe gives rise to additional signals and repetitive DNA sequences on other chromosomes. Small arrows indicate the position of AAV-2 DNA integrated into host DNA, comparable to panel A. The positions of chromosomes 19 visible by use of the painting probe are indicated with carets.

many. Biotinylated chromosome 17-specific human alpha satellite DNA was obtained from Oncor.

Denaturation and hybridization were performed directly with the hybridizing solution (see below) on the slide under a siliconized coverslip sealed with glass coverslip sealant from Oncor. Biotin-labeled probes were denatured and hybridized in the presence of 50% deionized formamide–0.5× Denhardt's solution (Serva)–10% dextran sulfate–100 μg of sonicated salmon sperm DNA per ml–2× SSC in a final concentration of 250 ng/ml. Then, 20 μl of the solution was added to each slide. Chromosomal and probe DNA were denatured by placing the slides onto a heated plate for 4 to 6 min at 92 to 94°C. After denaturation, the slides were incubated in a moist chamber (2× SSC and 50% formamide) for 16 h at 42°C. In a first step, hybridization with the AAV-2-specific probe and p53-specific probe was performed, followed by detection and mounting as described below. The slides were screened with a fluorescence microscope (see below) for specific signals. In a subsequent procedure, the slides were immersed in PBS at 37°C for at least 12 h to remove the coverslips and the sealant. This was followed by fixation in cold ethanol (−20°C) for 1 h. After being air-dried, the slides were hybridized with the chromosome 17-specific probe (chromosome 17-specific satellite DNA) (Oncor) as described above. With the second detection procedure (see below), the fixed biotin-avidin compounds specific for AAV-2 and p53 were increased in their intensity.

Biotinylated painting probes (chromosomes 17 and 19) and fixed chromosome preparations were denatured separately and hybridized together for 16 h (35, 43).

In situ detection. Washing and detection were done with the chromosome in situ kit obtained from Oncor. After removal of the sealing glue, preparations were transferred to postwashing solution (2× SSC, 56% deionized formamide) and incubated for 20 min at 43°C with occasional agitation. During this washing step, the coverslips fall off the slides. After two additional washings in 2× SSC (pH 7.0) at 37°C, each for 5 min, the slides were immersed in BPD buffer (from the kit) at room temperature. Slides were drained but not allowed to dry and then incubated with 60 μl of blocking buffer 1 for 5 min at room temperature, sealed with a flexible plastic coverslip to avoid distortion of the preparations by removal. Incubation with 60 μl of fluorescein isothiocyanate (FITC)-labeled avidin was carried out under the same coverslips in a moist chamber (2× SSC) at 37°C for 20 min. After removal of the coverslips, the slides were washed three times in BPD buffer at room temperature for 2 min. Before the following amplification step with a biotin-antiavidin antibody, the slides were again incubated with a blocking reagent (60 μl) for 5 min at room temperature. The incubation with 60 μl of FITC-labeled avidin for 20 min in a moist chamber (2× SSC) was followed by three washes with BPD buffer for 2 min each. The slides were then again incubated with 60 μl of blocking buffer, sealed with a plastic coverslip, for 5 min at room temperature. Excess liquid was tapped off, and 60 μl of avidin–FITC-labeled antibiotin complex was added to each slide, sealed with a plastic coverslip, and incubated at 37°C in a moist chamber for 20 min. After removal of the coverslips, the slides were washed in BPD buffer at room temperature three times for 2 min each. Before being mounted with Antifade (18 μl per slide; Oncor), the slides were counterstained with propidium iodide diluted in BPD buffer to a final concentration of 100 ng/ml for 5 min.

After simultaneous hybridization with painting probes and Digoxigenin-labeled AAV-2 DNA, the slides were washed four times for 5 min each in 50% formamide–2× SSC at 45°C. Then the slides were transferred to a Coplin jar containing 0.1× SSC warmed to 60°C. After three washes for 5 min each, the slides were equilibrated in BPD buffer. Detection was performed either with FITC-avidin (Dianova, Hamburg, Germany) or with rhodamine-antidigoxygenin antibody (Boehringer). In the case of rhodamine, we used 4',6-diamidino-2-phenylindole as a counterstain.

Preparations were examined with a DIALUX 22/22 EB microscope (Leitz, Wetzlar, Germany) with epi-illumination from an HBO 200-W mercury arc (Osram). The FITC fluorescence was visualized with a BP 450-490 excitation and an LP 515 emission filter combination with an RKP 510 dichroic mirror. For the red propidium iodide fluorescence, a BP 530-560 excitation and an RKP 580 emission filter combination with a 580-nm dichroic mirror were used. Photographs were taken on AGFA-P800/1600 films (24 by 36 mm) with exposure at ASA 1600.

Treatment with cytotoxic and genotoxic agents. HeLa and HA-3x, HA-16, and HA-28 cells were seeded on 100-mm plastic petri dishes at a concentration of 10^5 cells per dish. After 8 h, MNNG or DMBA was added to the medium at a final concentration of 50 or 20 mM, respectively. Similarly, cells were treated with recombinant human tumor necrosis factor alpha in a final concentration of 500 ng/ml or were incubated at 42°C for 45 min. Cultures were then incubated at 37°C in a humidified atmosphere with 5% CO_2. Phase contrast micrographs were taken at the times indicated in the figure legends.

Colony-forming ability. The plating efficiency of HeLa cells and AAV DNA-containing HeLa-derived clones was determined by plating 100 or 500 cells of treated (as above) or untreated cultures and counting the number of outgrowing clones after fixation with 4% formaldehyde and staining with crystal violet (Fluka, Buchs, Switzerland).

Soft-agar cloning. A 2% stock solution of soft agar (Bacto

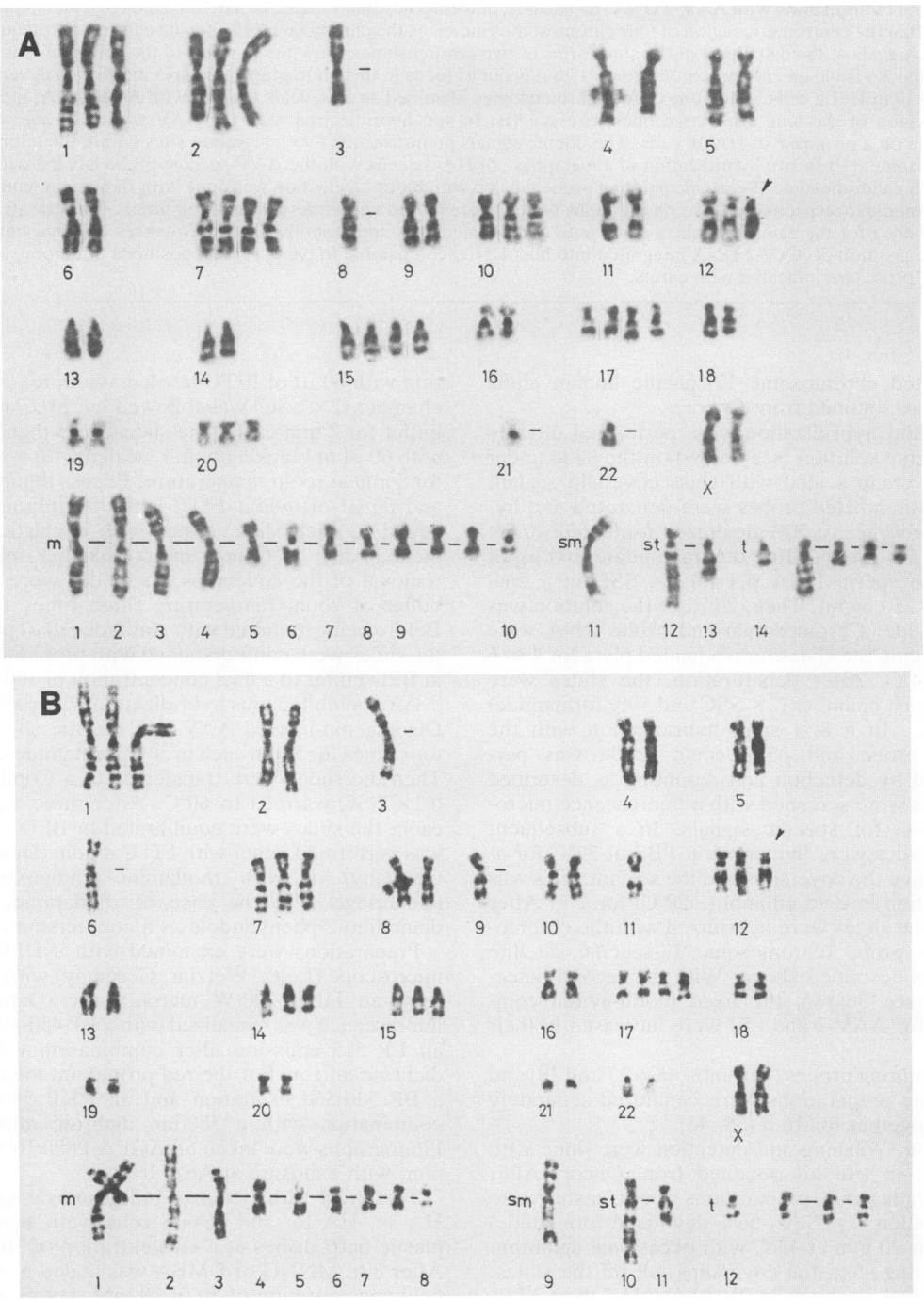

FIG. 3. (A) Representative G-banded karyotype of cells of the HA-3x clone, illustrating the presence of 14 marker chromosomes along with 4 structurally abnormal chromosomes (last row). (B) Representative G-banded karyotype of the HA-16 cell clone, showing 12 marker chromosomes along with 3 structurally abnormal chromosomes. The arrows indicate a chromosomal deletion, del(12)(p11:), regularly found in both clones and in the parental HeLa cell line.

Agar; Difco, Hamburg, Germany) in water was autoclaved for 15 min at 121°C. The agar was cooled down to 45°C. DMEM, twofold-concentrated (2×) DMEM, and FCS were warmed to 45°C. The "base layer" was prepared by adding 25 ml of 2× DMEM, 30 ml of DMEM, 20 ml of FCS, and 25 ml of agar stock solution (2%); 15 ml of this base layer (0.5% agar) was poured into 10-cm petri dishes. The dishes were placed with the lids open under a laminar flow hood for 15 min and for another 15 min with closed lids in a 4°C room to allow the agar to solidify. Then 500 cells (suspended in 0.8 ml of DMEM without FCS) were added to 1.2 ml of the base layer mix. The cell suspensions (0.3% agar) were carefully laid onto the basal agar. Prior to incubation in an incubator (5% CO_2, 37°C), the dishes were allowed to cool at room

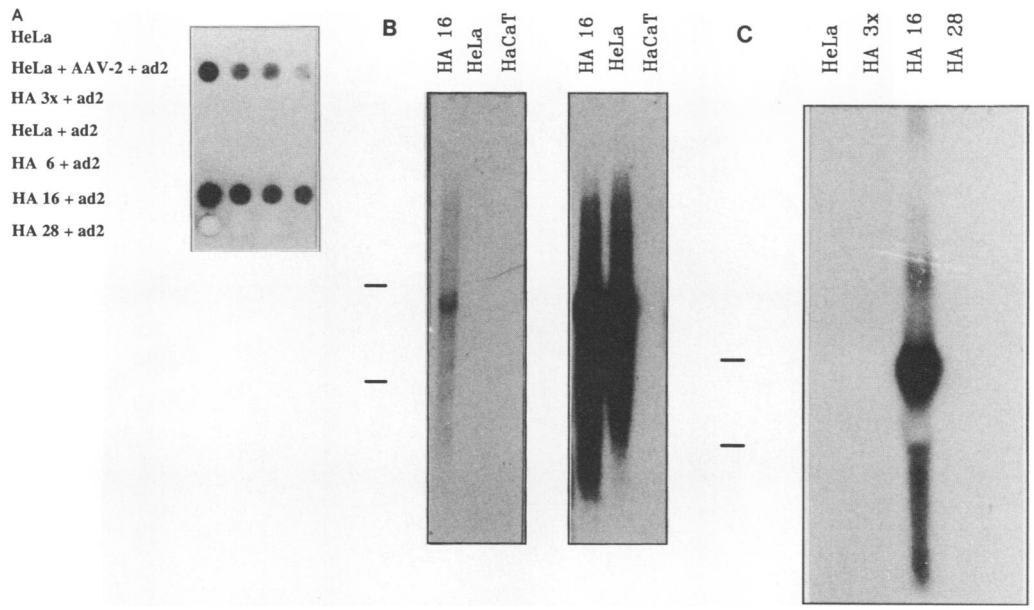

FIG. 4. (A) Rescue of infectious AAV-2 particles from cellular clones with integrated AAV-2 DNA. Parental HeLa cells and HeLa cells coinfected with AAV-2 and adenovirus type 2 (ad2) served as positive controls (AAV-2, MOI = 10 PFU/cell; ad2, MOI = 100 PFU/cell). The cellular clones HA-3x, HA-6, HA-16, and HA-28 as well as the parental HeLa cell line were infected with ad2 (1 PFU/cell). After completion of CPE, cells were harvested, disrupted by freezing and thawing, and then centrifuged. Supernatants were incubated at 60°C for at least 1 h to inactivate adenovirus, and aliquots were diluted from 10^{-1} to 10^{-15}. Aliquots were inoculated onto HeLa cells in 96-well plates together with adenovirus (MOI = 10 PFU/cell). After reaching complete CPE, cells were harvested and transferred to a nitrocellulose filter with a dot-blot apparatus. After immobilization, denaturation, and renaturation, filters were hybridized with radiolabeled AAV-2 DNA. The lane with the supernatant from HeLa cells shows no positive dots, as does the fourth lane with the supernatant from HeLa cells superinfected with adenovirus (control). Supernatants from HeLa cells coinfected with AAV-2 and adenovirus as a helper generated infectious AAV-2 particles, as shown by the positive dots in the second lane. Of the cellular clones with integrated AAV-2 DNA, only HA-16 produced infectious AAV-2 particles after infection with adenovirus. (B) Northern blot analysis of cells of clone HA-16, of the parental HeLa cell line, and of the keratinocyte cell line HaCaT. A total of 5×10^7 cells of each cell line were lysed in guanidinium thiocyanate. Poly(A)$^+$ mRNA was prepared with the Fast Track mRNA Isolation Kit. Samples of RNA (10 μg each) were separated by electrophoresis through a 1% agarose gel in MOPS buffer at 60 V for 5 h. RNA was transferred to a Gene-Screen, immobilized, and hybridized with [α-^{32}P]dTTP-labeled AAV-2 DNA (left *Bam*HI fragment of the viral genome) (left blot), followed by probe removal and rehybridization with [α-^{32}P]dTTP-labeled HPV-18 DNA (right blot). Size markers indicate the size of the human 28S rRNA (upper marker; 4,850 bases) and 18S rRNA (lower marker; 1,850 bases). Among all the clones tested, only in HA-16 cells could AAV RNA be detected (after exposure for 7 days). The size of the RNA fragment, about 4.2 kb, suggests transcription of the early (*rep* 78) RNA of AAV-2. HeLa cells (uninfected parental cell line) show no signal, nor does the negative control (HaCaT cells). Rehybridization with radiolabeled HPV-18 DNA revealed basal transcription of the HPV-18 E6 and E7 open reading frames characteristic of HeLa cells. (HaCaT cells contain no known viral DNA.) (C) Northern blot analysis of the cellular clones HA-3x, HA-16, and HA-28 and of HeLa cells 12 h after superinfection with adenovirus type 2 as the helper virus. From each cell line, 10^6 cells were harvested, and total cellular RNA was extracted by the acid-guanidinium-thiocyanate-phenol-chloroform extraction method. RNA (10 μg) was separated by agarose gel electrophoresis (1% agarose) in MOPS buffer, blotted onto a nylon membrane (Gene-Screen), and hybridized with [α-^{32}P]dTTP-labeled AAV-2 DNA. The markers represent 4.805 kb (human 28S rRNA) and 2.0 kb (human 18S rRNA). After exposure for 12 h, strong signals of RNA (4.2 kb) were detectable in the HA-16 lane. Even after extended exposure (7 days), no signals were detected on blots of RNA of the other cell lines. At the time of RNA extraction (12 h after adenovirus infection), no HPV-18 transcription could be found in the cell lines (host cell shut-off by adenovirus).

temperature. The size and number of colonies were determined after 3 weeks.

Rescue of infectious AAV-2 particles. To determine whether AAV-2 could be rescued from its integrated state in HA-3x, HA-16, and HA-28, cells were superinfected with adenovirus type 2 (1 PFU per cell). After completion of adenovirus-induced CPE, the cells were disrupted by freezing and thawing. After centrifugation, the supernatant was incubated at 60°C for 1 h to inactivate helper virus. Aliquots were diluted from 10^{-1} to 10^{-15} and inoculated on 96-well plates together with adenovirus (MOI, 10 PFU per cell). After CPE was complete, the cells were harvested and transferred to nitrocellulose filters (Schleicher & Schüll, Dassel, Germany) with a dot-blot apparatus (Minifold-1; Schleicher & Schüll). The presence of AAV-2 progeny particles was determined by hybridizing the filters (dispersed-cell assay) with radiolabeled AAV-2 DNA.

Growth of HeLa cells and AAV DNA-containing HeLa-derived clones in nude mice. Female immunodeficient (nude) mice (CD1 *nu/nu*, 7 weeks old), purchased from Charles River WIGA (Sulzfeld, Germany), were housed (five per cage) in isolators and received normal food and water. For each experimental protocol (control and irradiation; see below), five animals were examined. Cells (10^6 in 100 μl of PBS) of HeLa, HA-3x, HA-16, and HA-28 from exponentially growing cell cultures were injected subcutaneously into the right flank of the animals.

The region of the animals where tumors were growing was exposed to gamma rays 2 weeks after inoculation of cells (10 Gy; source to surface distance, 70 cm) with a Gammatron II

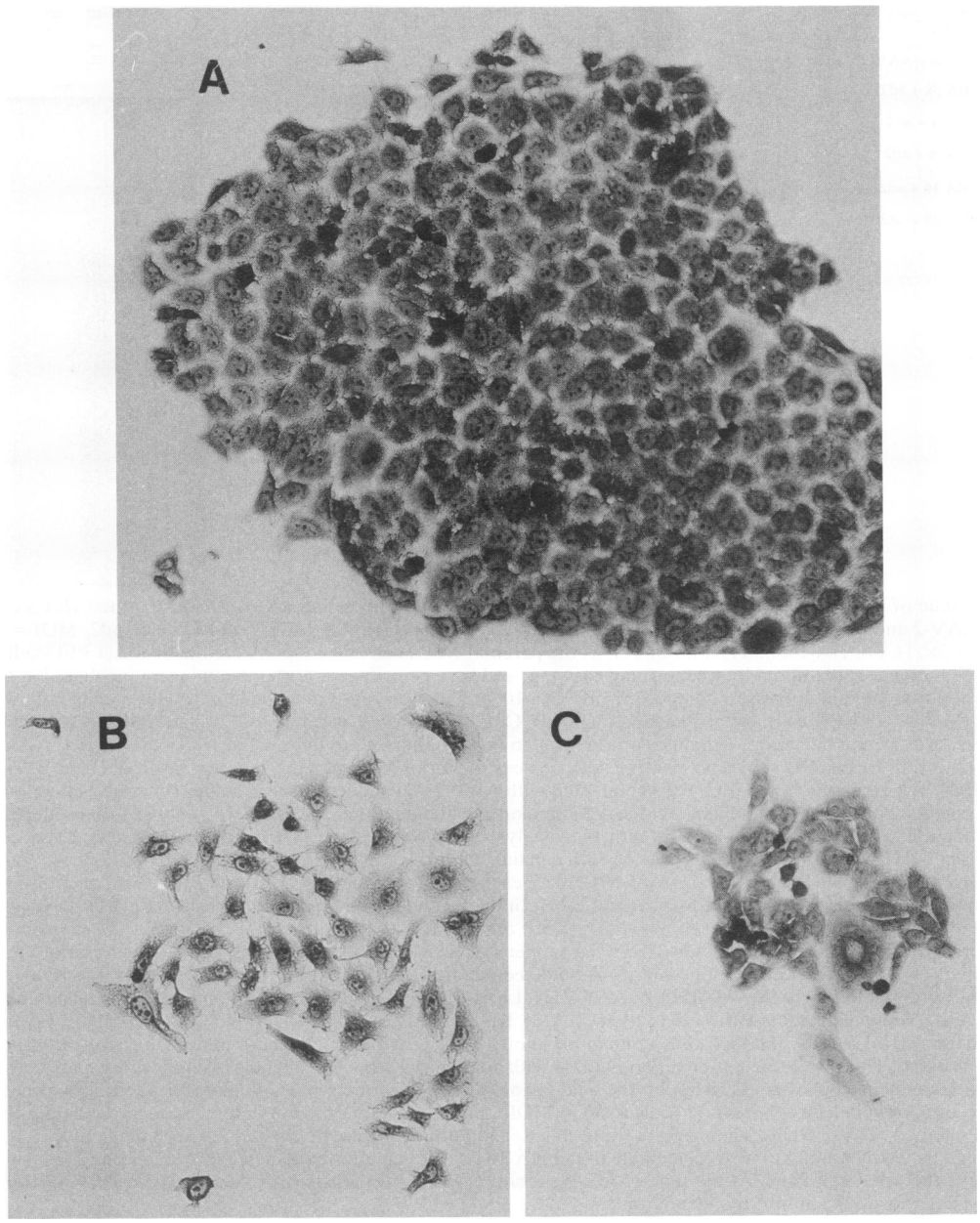

FIG. 5. Plating morphology of HeLa[AAV$_i$] clones. Cell clones containing AAV DNA revealed reduced growth rate and smaller colonies. Photographs were made of colonies stained with crystal violet after plating onto petri dishes for elucidation of plating efficiency (see Table 1). The micrographs show a comparison between colonies of HeLa and HA-16 cells after growth for 6 days. Colonies of HA-16 (b) and HA-3x (c) cells show altered growth behavior compared with colonies of HeLa cells (a). The intercellular space between cells of the AAV DNA-containing clones is enlarged, whereas colonies of HeLa cells are formed by very tightly growing cells.

(Siemens, Munich, Germany). Prior to irradiation, the animals were anesthesized with Ketavet (0.3 mg per animal) (Parke-Davis, Berlin, Germany) and Rompun (1.5 mg per animal) (Bayer, Leverkusen, Germany). Nonirradiated animals were kept as controls.

The growth rate of tumors was determined by weekly measuring of two diameters of individual tumors. After 48 days, the animals were killed, and tumor tissue was removed and frozen in liquid nitrogen. From these samples, DNA and RNA were extracted and processed as described above.

RESULTS

Physical analysis of integrated AAV-2 DNA in HeLa cells. From HeLa cells infected with AAV-2 and passaged twice before being seeded as single cells, 50 colonies were isolated which were analyzed by the dispersed-cell assay (61) for the presence of AAV DNA. Figure 1A shows that different numbers of AAV genomes were present in the clones. Three of 11 positive cellular clones were analyzed further: HA-28, with one copy of AAV DNA, and HA-3x and HA-16, both

with more than 10 copies. The copy number was confirmed by Southern blot analysis of DNA from the cell clones (data not shown). In addition, AAV DNA-negative clones confirmed by Southern blot analysis were assayed for growth behavior (see below).

Restriction enzyme analysis of DNA from HA-28, HA-3x, and HA-16 (Fig. 1B, HA-16 as an example) revealed the presence of AAV DNA in an integrated state. Analysis by double digestion with restriction enzymes showed that the integration pattern is head-to-tail in HA-3x and HA-16. The restriction pattern of HA-28 revealed the loss of one cleavage site for *Sma*I at one of the terminal repeat sequences. It is known that integration of AAV DNA is frequently accompanied by alterations within the viral terminal repeats (31). Four more clones (HA-12, HA-14, HA-17, and HA-23), which have not yet been analyzed in detail, could be shown to have AAV DNA molecules in an integrated state which was different for all clones (i.e., no consistent pattern in restriction enzyme analysis). None of the clones revealed episomal AAV DNA (data not shown).

In view of the reported site-specific integration of AAV DNA (32, 33, 51) we performed in situ hybridization on metaphase spreads to analyze the integration site of the AAV DNA in the HeLa cell clones (designated HeLa[AAV_i] clones). In situ hybridization with AAV-specific probes of metaphases of HA-3x, HA-16, and HA-28 revealed that most molecules of AAV DNA had integrated at the distal part of the long arm of chromosome 17. The chromosomal location was confirmed by subsequent hybridization of the same metaphase with chromosome 17- and chromosome 19-specific probes (centromeric region and painting probe, respectively) as well as by additional hybridization with a probe specific for the p53 gene, which is located at the short arm of chromosome 17 (4, 39, 40) (Fig. 2A, HA-3x). Interestingly, in situ hybridization with p53 DNA revealed p53-specific sequences only at three of the four chromosomes 17 present in HeLa cells (Fig. 2A). In situ hybridization on chromosomal spreads with prophase and metaphase chromosomes pointed to at least two integration sites of AAV DNA, in accordance with the number of offsize signals in Southern blots of HA-3x and HA-16 DNA (Fig. 2B, HA-16). Similarly, in accordance with Southern blot analysis of clone HA-28 indicating integration of only one genome of AAV, in situ hybridization of metaphases of these cells resulted in a rather weak signal on 17q (data not shown). In order to exclude translocation of chromosome 19-specific sequences to chromosome 17, we performed double in situ hybridization with AAV DNA and chromosome 19-specific painting probes. There are problems in hybridization and washing conditions when using AAV DNA (few copies integrated) and a painting probe containing repetitive sequences simultaneously because repetitive regions of other chromosomes also become labeled. In spite of this "background" problem, it is clear from Fig. 2C that signals from the chromosome 19-specific painting probes always lit up at chromosomal structures distant from AAV signals, supporting the finding of an association of AAV DNA with chromosome 17.

In view of the finding of integration of AAV DNA into chromosome 17 in all three HeLa[AAV_i] clones, we performed cytogenetic analyses to ascertain the individuality of the clones. Karyotype analysis of cells from early passages of HA-3x and HA-16 confirmed the independent origin of the clones. The cells of the HA-3x clone (Fig. 3A) displayed an average chromosome number of 74 (70% of the metaphases), with variations from 66 to 75. The 15 marker chromosomes observed were present at one copy per cell, with the exception of marker chromosome 9 (frequently three copies). The chromosome number of HA-16 cells (Fig. 3B) was 67 (average; 56% of the metaphases), varying from 66 to 69, with 12 marker chromosomes. Marker chromosomes were found in a single copy except for marker chromosome 7. (HA-28 could be distinguished from HA-3x and HA-16 by Southern blot analysis, as described above. It is interesting that karyotype analysis revealed two chromosomes 19, whereas in in situ hybridization [Fig. 2C], three chromosomal structures were labeled with the chromosome 19-specific painting probes. Apparently, some rearranged sequences of chromosome 19 were not detectable in conventional karyotype analyses.)

TABLE 1. Plating efficiency of HeLa-derived cellular clones containing AAV-2 DNA compared with that of cells of the parental HeLa cell line[a]

No. of cells plated	No. of outgrowing colonies (mean ± SD)			
	HeLa	HA-3x	HA-16	HA-28
100	81.5 ± 1.5	78.5 ± 3.5	13.0 ± 5.0	48.0 ± 6.0
500	407.5 ± 42.4	324.3 ± 60.3	126.0 ± 78.4	200.0 ± 2.5

[a] Reduced plating efficiency of AAV-2 DNA-containing HeLa-derived cellular clones HA-16 and HA-28. Cells of semiconfluently growing HA-3x, HA-16, HA-28, and HeLa cell cultures were harvested and seeded at 100 and 500 cells onto 10-cm plastic petri dishes. Cultures were grown at 37°C in 5% CO_2 humidified atmosphere for 7 days. Cells were then fixed with 4% formaldehyde and stained with crystal violet, and the mean number of outgrowing colonies from three different experiments was determined.

Additional evidence for the individuality of HeLa[AAV_i] clones is presented by the following results.

Transcription from integrated AAV DNA and rescue of infectious virions. It has been reported by others (13, 23, 33, 41, 49, 50) that integrated AAV DNA can be rescued to yield infectious virions by superinfection with helper virus. Superinfection of HA-3x, HA-16, and HA-28 with adenovirus type 2 revealed different rescuability of the integrated genomes (Fig. 4A). HA-16 efficiently produced infectious AAV particles after infection with adenovirus, whereas no rescue of AAV infectivity could be obtained from adenovirus-infected HA-28 or HA-3x cells. This suggests deletions within the AAV DNA molecules in HA-28 (see above) and HA-3x, which in HA-3x were not detectable by restriction enzyme analysis.

Northern (RNA) blot analyses of AAV-specific mRNAs [poly(A)$^+$-selected transcripts] in the three HeLa[AAV_i] clones demonstrated AAV-specific transcripts only in HA-16 (Fig. 4B). This is reflected also by the enhanced transcript levels observed after superinfection with adenovirus (Fig. 4C). The size of the transcript as well as the probe used for detection (left part of the AAV genome [1,045-bp *Bam*HI fragment]) indicates transcription of early genes. However, AAV transcripts were not found after superinfection of HA-3x and HA-28 clones with adenovirus (Fig. 4B).

Biological properties of HeLa cells with integrated AAV DNA. In order to investigate whether integration of AAV DNA has biological consequences, we analyzed several cytological aspects of the HeLa[AAV_i] clones.

(i) Growth properties of HeLa[AAV_i] clones. Comparing the growth kinetics of HeLa cells and HeLa[AAV_i] clones revealed a slightly but constantly reduced growth rate. Among cells seeded at the same density, differences in the doubling of the cell populations were evident after a few passages. The kinetics revealed a constant reduction of the slope of the growth curve compared with that of HeLa cells

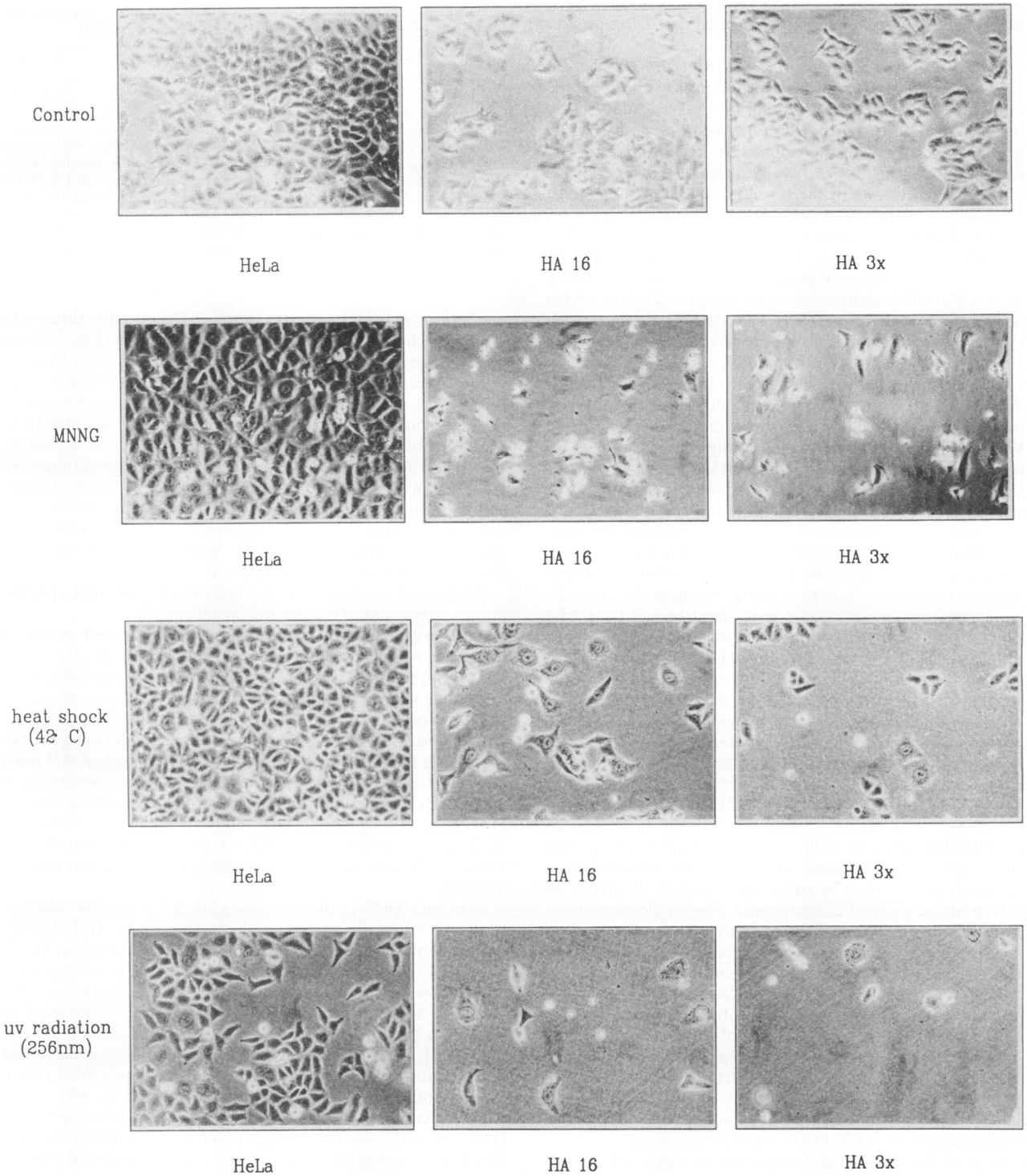

FIG. 6. (A) Growth of HeLa-derived cellular clones HA-3x and HA-16 and of the parental HeLa cell line after treatment with the genotoxic agent MNNG (50 mM), UV irradiation (10 J/m^2), and heat (42°C for 45 min) compared with that of untreated control cells. Cells were treated after reaching semiconfluency on a 10-cm plastic petri dish. The cytotoxic effect of MNNG is visible in AAV DNA-containing cellular clones 12 h after treatment, whereas HeLa cells were not affected. Heat-exposed or UV-treated HA-3x and HA-16 cells revealed toxic changes 48 h after treatment.

(data not shown). Two HeLa-derived clones which were negative for AAV DNA after selection displayed the same growth properties as the parental nonclonal HeLa cells (data not shown). The reduction of the growth rate for HeLa[AAV$_i$] clones was also evidenced by the different sizes of colonies from cells seeded at low density (500 cells per 10-cm dish) compared with the sizes of colonies of the parental HeLa cells (after 7 days of growth) (Fig. 5A and B). Microscopically, colonies of HeLa[AAV$_i$] clones revealed in addition an altered growth pattern, displaying increased intercellular space (Fig. 5A and B). Furthermore, the cloning efficiency was reduced for HA-16 and HA-28; however, HA-3x was an exception when numbers of colonies were considered (Table 1). The growth rate of cells of clone HA-3x was found to be reduced similar to that of cells of clones HA-16 and HA-28 when the smaller size of colonies compared with HeLa cell colonies was considered (Fig. 5C). Similarly, the ability to form colonies in semisolid medium was reduced (<50%) in all three HeLa[AAV$_i$] clones compared with the parental HeLa cell line (data not shown). In addition, HA-3X, HA-16, and HA-28 were not able to replicate at a serum concentration of 0.5% in the growth medium, in contrast to HeLa cells (data not shown).

(ii) Sensitivity of HeLa[AAV$_i$] clones to genotoxic stress. The most striking biological change in HeLa cells after integration of AAV DNA was the sensitivity of these cells to genotoxic agents. At concentrations of the carcinogens MNNG (50 mM) and DMBA (20 mM) at which HeLa cells were not affected, AAV DNA-containing cells died within 1 day after treatment (Fig. 6). Similarly, irradiation with UV light (10 J/m^2) or exposure to 42°C for 30 min led to premature cell death of HeLa[AAV$_i$] clones compared with HeLa cells (Fig. 6). Similar results were obtained after irradiation with gamma rays (data not shown). Furthermore, treatment with tumor necrosis factor alpha killed the HeLa[AAV$_i$] clones at doses (500 ng/ml) which were not toxic for cells of the HeLa line (data not shown). In addition, we could not find any increased sensitivity of cells of AAV DNA-negative clones (HA-14, HA-21, and HA-26) to treatment with MNNG and UV irradiation. After treatment with these agents, no enhancement of AAV transcription or amplification of AAV DNA could be found (data not shown).

(iii) Sensitivity of HeLa[AAV$_i$] clones to parvovirus H-1. It has been reported that malignant transformation sensitizes cells to the lytic effect of the autonomous parvoviruses H-1 and minute virus of mice (11, 12, 16, 47). Hence, sensitivity to these viruses might be considered a marker for the transformed phenotype. Therefore, we tested the sensitivity of HeLa[AAV$_i$] clones to H-1 infection. It could be shown that HeLa[AAV$_i$] clones displayed CPE from H-1 later than HeLa cells. HeLa cells were killed within 2 days, whereas HeLa[AAV$_i$] clones were not lysed until 4 days after infection with H-1 (data not shown).

(iv) Properties of HeLa[AAV$_i$] clones in vivo. In order to check these in vitro findings, we inoculated HeLa cells as well as HeLa[AAV$_i$] clones (HA-3x and HA-16) into nude mice. As shown in Fig. 7, tumors established from HeLa [AAV$_i$] clones grew more slowly than HeLa-derived tumors and were highly susceptible to irradiation with gamma rays. The reduced growth rate and enhanced susceptibility to genotoxic stress in vivo parallel the in vitro findings described above.

Southern blot analysis of DNA extracted from tumor tissues from irradiated and nonirradiated animals revealed no gross rearrangements of the integrated AAV DNA during growth in vivo. Similar to the results in cell culture, AAV

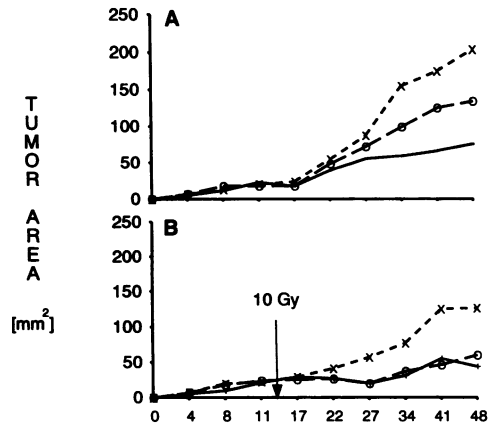

FIG. 7. Growth in vivo of tumors from HeLa cells (×) and from AAV DNA-containing HeLa cell clones HA-3x (–+–) and HA-16 (○). (A) Cells (5 × 10^5 in 100 μl of PBS) were injected subcutaneously into nude mice at day 0. Tumor growth was elucidated by measuring two diameters of each tumor to determine the tumor size. (B) To analyze the sensitivity of cells with integrated AAV DNA to cytotoxic agents in vivo, tumors from one group of animals were irradiated with gamma rays (10 Gy) at day 14. After irradiation, cells with integrated AAV DNA displayed an increased sensitivity to gamma rays.

transcripts could not be detected (Northern blot analysis) in tumor tissues of animals and were not induced by irradiation (data not shown). This again parallels our findings in cell culture (see above).

Transcription of HPV-18 in HeLa[AAV$_i$] clones. HeLa cells contain integrated HPV-18 DNA (8). The expression of these viral genes is linked to the transformed phenotype of this cervical carcinoma cell line (58). Therefore, we analyzed whether integration of AAV DNA into the genome of HeLa cells would influence the arrangement of DNA or the expression of HPV. The integration pattern of HPV-18 DNA was found to be unchanged (data not shown), and transcription of HPV genes was not altered in the cells with integrated AAV DNA (Fig. 8A). The level and pattern of transcripts of HPV found in HeLa cells and in HeLa[AAV$_i$] clones also remained unchanged after treatment of HeLa[AAV$_i$] clones with the genotoxic agents mentioned above (Fig. 8B).

DISCUSSION

We report here the consequences of integration of AAV DNA into the human cervical carcinoma cell line HeLa. HeLa-derived cellular clones containing AAV DNA (HeLa [AAV$_i$] clones) are downregulated in their growth properties in vitro as well as in vivo. HeLa[AAV$_i$] clones grow more slowly and require higher serum levels than the parental HeLa cells, paralleling findings on AAV-infected normal and malignant human cells (1, 3). The reduced growth rate was confirmed by in vivo experiments showing reduced growth of tumors established from these clones (in immunodeficient nude mice) compared with tumors from the parental HeLa cells. In addition, HeLa-derived clones with integrated AAV DNA were found to be sensitized to the effects of genotoxic influences: enhanced cell killing (compared with the HeLa cell line) could be observed after treatment of the HeLa[AAV$_i$] clones with MNNG or tumor necrosis factor alpha

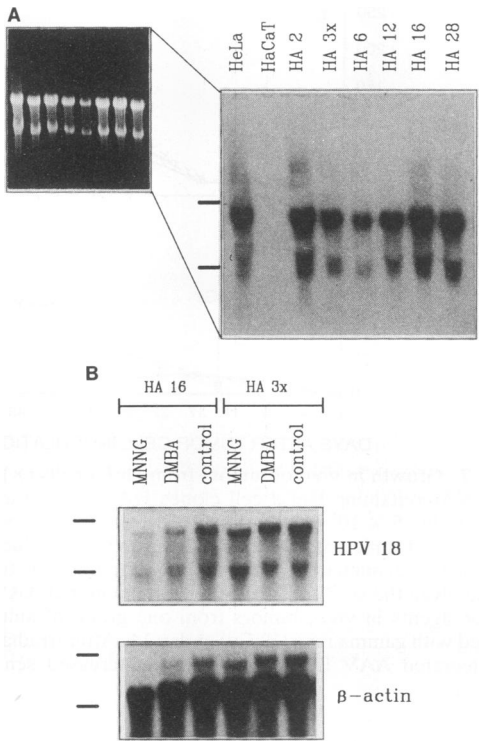

FIG. 8. Northern blot analysis of transcription of HPV-18 in the HeLa-derived clones with AAV-2 DNA integrated in the genome compared with that in parental HeLa cells and in cells of the human keratinocyte line HaCaT (negative control). Total cellular RNA was extracted by the acid guanidinium thiocyanate-phenol-chloroform extraction technique. RNA (10 μg per lane) was separated by electrophoresis through a 1% agarose gel in MOPS buffer, blotted to a nylon membrane (Gene-Screen), and probed with radiolabeled HPV-18 DNA. Markers indicate the size of human 28S rRNA (4.805 kb) and human 18S rRNA (2.0 kb). (A) Compared with the relative amounts of RNA loaded onto the gel (ethidium bromide staining of the gel; left), the hybridization signals revealed no alteration of HPV-18 transcription after integration of AAV DNA into the genome of HeLa cells. (B) Northern blot analysis of total cellular RNA of the HeLa-derived cellular clones HA-16 and HA-3x, 8 h after treatment with MNNG (50 mM) and DMBA (20 mM). RNA was extracted by the acid guanidinium thiocyanate-phenol-chloroform extraction method. Ten micrograms of RNA from each sample was separated through a 1% agarose gel in MOPS buffer, blotted to a nylon membrane (Gene-Screen), and hybridized with [α-^{32}P]dTTP-labeled HPV-18 DNA and subsequently with [α-^{32}P]dTTP-labeled β-actin DNA to compare the amounts of RNA loaded per track. Markers indicate the positions of human 28S rRNA (4.805 kb) and human 18S rRNA (2.0 kb). Hybridization reveals no alteration of HPV-18 transcription after treatment with the drugs.

and irradiation of the cells with UV light or gamma rays as well as by short incubation of the cells at 42°C (heat shock).

It has been shown that AAV-2 infection can lead to perturbation of the cell multiplication sequence by inducing cell cycle arrest in the G2 phase (2, 3, 60). Possibly, some stages of the cell cycle are disturbed in AAV DNA-containing cells. This might involve prolongation of stages in which cells are particularly sensitive to genotoxic stress. Also, tumors derived from HeLa[AAV$_i$] clones displayed an enhanced sensitivity to gamma irradiation compared with tumors established from HeLa cells. The alteration of growth properties and the sensitization to (genotoxic) stress seem to be independent of the number of integrated AAV DNA copies or of efficient transcription and expression of parvoviral genes. There is no significant expression of AAV genes (as detectable by Northern blot and Western immunoblot analysis) either in vitro or in vivo in the AAV DNA-containing clones (with the exception of a very weak transcription of the *rep* gene in HA-16). Also, after treatment with cytotoxic agents, expression of AAV genes was not induced. It might be possible that integrated AAV DNA structures play a role in the alteration of biological properties of the clones described here. It has been shown that AAV DNA (especially sequences of the AAV origin of replication [*ori*] and of the terminal repeats) can interact with cellular factors. By Southwestern (DNA-protein) blot analysis, four different nuclear proteins with increased affinity to the *ori* region or specific regions within the terminal repeats of AAV DNA could be identified after treatment with MNNG (63). These finding were confirmed by band shift analysis. Dirschnabel reports a comparable affinity of simian virus 40 core *ori* and sequences of the regulatory region of c-*myc* for these DNA-binding proteins (20). It might therefore be possible that DNA-binding proteins play a role in the phenotypic alterations of cells containing AAV DNA.

It will be necessary to clarify the significance of our observation that AAV DNA is integrated essentially at sites on the long arm of chromosome 17 (in the three representative cellular clones HA-3x, HA-16, and HA-28). Whether this points to integration sites in HeLa cells involving specific genes is currently under investigation. Integration into chromosome 17 is at variance with the results of other reports on frequent integration of AAV DNA in chromosome 19 in different human cell lines (32, 33, 51). It has not been reported whether these cells also show phenotypic alterations. Hence, the available data probably point to preferential rather than to specific (unique) integration sites for AAV (possibly depending on the infection protocol and the cell lines investigated).

Our observations on tumor cells with integrated AAV DNA hint to a partial reversion of the transformed phenotype (e.g., enhanced serum requirement, increased space between attached cells, reduced colony formation in semisolid medium, and reduced tumor growth in animals) accompanied by an enhanced sensitivity to toxic agents. This is further stressed by a reduced sensitivity of HeLa[AAV$_i$] clones to the cytolytic effect of parvovirus H-1. The permissiveness of cultured cells to H-1 CPE seems to indicate a transformed phenotype of the cells (11, 12, 16, 45).

Serological findings suggest a reduced cancer risk for individuals latently infected with AAV (see the introduction). Considering the enhanced sensitivity of HeLa[AAV$_i$] clones to genotoxic stress in vitro and in vivo, it is tempting to speculate that populations of cells with integrated AAV DNA emerging after natural infection would be more sensitive to genotoxic hits. Such hits are supposed to take place sequentially in a cell on its way to full tumorigenic transformation (36). According to our observation, cells with integrated AAV DNA would possibly be killed preferentially by genotoxic events, thus reducing the probability of such cells becoming transformed. To substantiate this hypothesis, it will be necessary to establish whether integration of AAV DNA also occurs in natural infections and whether specific target cells or organs can be identified.

Sensitization of cells to genotoxic stress has also been observed shortly after infection of culture cells with AAV (2, 25). Whether this phenomenon involves integration of AAV DNA remains to be determined. In addition, it will be necessary to investigate whether infection of tumor cells in

vivo leads to integration of AAV DNA. Since integration of the DNA of this nonpathogenic virus influences the growth rate of tumors as well as enhances the sensitivity of tumor cells to "toxic" treatment or irradiation, this could give rise to novel concepts in cancer treatment.

ACKNOWLEDGMENTS

We thank N. E. Fusenig for providing the HaCaT cell line, E. Schwarz for cloned HPV-18 DNA and β-actin DNA, C. Laughlin for plasmid pAV2, L. V. Crawford for cloned p53 DNA, and P. Lichter for the painting probes for chromosomes 17 and 19. We are grateful to A. Mincheva for karyotyping of the cellular clones. We thank H. zur Hausen for constant support and many helpful discussions. We further thank E. Schwarz for critical reading of the manuscript.

This work was supported by grant Schl203/3-2 from the Deutsche Forschungsgemeinschaft.

REFERENCES

1. **Bantel-Schaal, U.** 1990. Adeno-associated parvovirus inhibit growth of cells derived from malignant human tumors. Int. J. Cancer **45:**190–194.
2. **Bantel-Schaal, U.** 1991. Infection with adeno-associated parvovirus (AAV) leads to increased sensitivity of mammalian cells to stress. Virology **182:**260–268.
3. **Bantel-Schaal, U., and M. Stöhr.** 1992. Influence of adeno-associated virus on adherence and growth properties of normal cells. J. Virol. **66:**773–779.
4. **Benchimol, S., P. Lamb, L. V. Crawford, D. Sheer, T. B. Shours, G. A. P. Bruns, and J. Peacock.** 1985. Transformation associated p53 protein is encoded by a gene on human chromosome 17. Somat. Cell Mol. Genet. **11:**505–509.
5. **Berns, K. I., and R. A. Bohensky.** 1987. Adeno-associated virus: an update. Adv. Virus Res. **32:**243–306.
6. **Berns, K. I., and W. W. Hauswirth.** 1979. Adeno-associated viruses. Adv. Virus Res. **25:**407–449.
7. **Blacklow, N. R., M. D. Hoggan, M. S. Sereno, C. D. Brandt, H. W. Kim, R. H. Parrot, and R. M. Chanock.** 1971. A seroepidemiologic study of adeno-associated virus infection in infants and children. Am. J. Epidemiol. **94:**359–366.
8. **Boshart, M., L. Gissmann, H. Ikenberg, A. Kleinheinz, W. Scheurlen, and H. zur Hausen.** 1984. A new type of papillomavirus DNA: its presence in genital cancer biopsies and in cell lines derived from cervical cancer. EMBO J. **3:**1151–1157.
9. **Boukamp, P., R. T. Petrusevsky, D. Breitkreuz, J. Hornung, A. Markham, and N. E. Fusenig.** 1988. Normal keratinization in a spontaneously immortalized aneuploid human keratinocyte cell line. J. Cell Biol. **106:**761–771.
10. **Casto, B. C., and C. R. Goodheart.** 1972. Inhibition of adenovirus transformation in vitro by AAV-1. Proc. Soc. Exp. Biol. Med. **140:**72.
11. **Chen, Y. Q., F. de Foresta, J. Hertoghs, B. L. Avalosse, J. J. Cornelis, and J. Rommelaere.** 1986. Selective killing of simian virus 40-transformed human fibroblasts by parvovirus H-1. Cancer Res. **46:**3574–3579.
12. **Chen, Y. Q., M. C. Tuynder, J. J. Cornelis, P. Boukamp, N. E. Fusenig, and J. Rommelaere.** 1989. Sensitization of human keratinocytes to killing by parvovirus H-1 takes place during their malignant transformation but does not require them to be tumorigenic. Carcinogenesis **10:**163–167.
13. **Cheung, A. K., M. D. Hoggan, W. W. Hauswirth, and K. I. Berns.** 1980. Integration of the adeno-associated virus genome into cellular DNA in latently infected human Detroit 6 cells. J. Virol. **33:**739–748.
14. **Chomczynski, P., and N. Sacchi.** 1987. Single-step method of RNA isolation by acid guanidinium thiocyanate-phenol-chloroform extraction. Anal. Biochem. **162:**156–159.
15. **Church, G. M., and W. Gilbert.** 1984. Genomic sequencing. Proc. Natl. Acad. Sci. USA **81:**1991–1995.
16. **Cornelis, J. J., B. L. Avalosse, S. Mousset, M. Namba, and J. Rommelaere.** 1986. Selective destruction by parvoviruses of human and mouse fibroblasts transformed with γ-irradiation. Int. J. Radiat. Biol. **49:**529.
17. **Cukor, G., N. R. Blacklow, D. Hoggan, and K. I. Berns.** 1984. Biology of adeno-associated virus, p. 33–66. *In* K. I. Berns (ed.), The parvoviruses. Plenum Publishing Corp., New York.
18. **Cukor, G., N. R. Blacklow, S. Kibrick, and I. C. Swan.** 1975. Effect of adeno-associated virus on cancer expression by herpesvirus-transformed hamster cells. J. Natl. Cancer Inst. **55:**957–959.
19. **de la Maza, L. M., and B. J. Carter.** 1981. Inhibition of adenovirus oncogenicity in hamsters by adeno-associated virus DNA. J. Natl. Cancer Inst. **67:**1323–1326.
20. **Dirschnabel, A.** 1990. DNA-Protein Bindungsstudien am Replikationsursprung und frühen Promotorbereich des Adeno-assoziierten Virus Typ 2: Charakterisierung kanzerogen-induzierter zellulärer DNA-bindender Proteine. Thesis. Ruprecht-Karls-Universität Heidelberg, Heidelberg, Germany.
21. **Feinberg, A., and B. Vogelstein.** 1984. A technique for radiolabeling DNA restriction endonuclease fragments to high specific activity. Anal. Biochem. **137:**266–267.
22. **Georg-Fries, B., S. Biederlack, J. Wolf, and H. zur Hausen.** 1984. Analysis of proteins, helper dependence and seroepidemiology of a new human parvovirus. Virology **134:**64–71.
23. **Handa, H., K. Shiroki, and H. Shimojo.** 1977. Establishment and characterization of KB cell lines latently infected with adeno-associated virus type 1. Virology **82:**84–92.
24. **Heilbronn, R., A. Bürkle, S. Stephan, and H. zur Hausen.** 1990. The adeno-associated virus *rep* gene suppresses herpes simplex virus-induced DNA amplification. J. Virol. **64:**3012–3018.
25. **Heilbronn, R., J. R. Schlehofer, and H. zur Hausen.** 1984. Selective killing of carcinogen-treated SV40-transformed Chinese hamster cells by a defective parvovirus. Virology **136:**439–441.
26. **Henry, C. J.** 1973. Adenovirus-associated (satellite) viruses. Prog. Exp. Tumor Res. **18:**273–293.
27. **Hermonat, P. L.** 1989. The adeno-associated virus rep 78 gene inhibits cellular transformation induced by bovine papillomavirus. Virology **172:**253–261.
28. **Hoggan, M. D., G. F. Thomas, F. B. Thomas, and F. B. Johnson.** 1972. Continuous "carriage" of adeno-associated virus genome in cell cultures in the absence of helper adenovirus, p. 243–249. *In* Proceedings of the Fourth Lepetit Colloquium, Cocoyac, Mexico. North-Holland Publishing Company, Amsterdam.
29. **Katz, E., and B. J. Carter.** 1986. Effect of adeno-associated virus on transformation of NIH 3T3 cells by ras gene and on tumorigenicity of an NIH 3T3 transformed cell line. Cancer Res. **46:**3023–3026.
30. **Kirschstein, R. L., K. O. Smith, and E. A. Peters.** 1968. Inhibition of adenovirus 12 oncogenicity by adeno-associated virus. Proc. Soc. Exp. Biol. Med. **128:**670–673.
31. **Kotin, R. M., and K. I. Berns.** 1989. Organization of adeno-associated virus DNA in latently infected Detroit 6 cells. Virology **170:**460–467.
32. **Kotin, R. M., J. C. Menninger, D. C. Ward, and K. I. Berns.** 1991. Mapping and direct visualization of a region-specific viral DNA integration site on chromosome 19q13-qter. Genomics **10:**831–834.
33. **Kotin, R. M., M. Siniscalco, R. J. Samulski, X. D. Zhu, L. Hunter, C. A. Laughlin, S. McLaughlin, N. Muzyczka, M. Rocchi, and K. I. Berns.** 1990. Site-specific integration by adeno-associated virus. Proc. Natl. Acad. Sci. USA **87:**2211–2215.
34. **Laughlin, C. A., C. B. Cardellichio, and H. C. Coon.** 1986. Latent infection of KB cells with adeno-associated virus type 2. J. Virol. **60:**515–524.
35. **Lichter, P., T. Cremer, L. Manuelidis, and D. C. Ward.** 1988. Delineation of individual human chromosomes in metaphase and interphase cells by in situ suppression hybridization using recombinant DNA libraries. Hum. Genet. **80:**224–234.
36. **Marks, F., and G. Fürstenberger.** 1987. Multistage carcinogenesis: the mouse skin model, p. 18–30. *In* H. zur Hausen and J. R. Schlehofer (ed.), The role of DNA amplification in carcinogenesis. J. B. Lippincott Co., Philadelphia.
37. **Mayor, H. D., S. Drake, J. Stahmann, and D. M. Mumford.** 1976. Antibodies to adeno-associated satellite virus and herpes

simplex in sera from cancer patients and normal adults. Am. J. Obstet. Gynecol. **126:**100–104.
38. **Mayor, H. D., G. S. Houlditch, and D. M. Mumford.** 1973. Influence of adeno-associated satellite virus on adenovirus-induced tumors in hamsters. Nature (London) New Biol. **241:** 44–46.
39. **McBride, O. W., D. Merry, and D. Givol.** 1986. The gene for human p53 cellular tumor antigen is located on chromosome 17 short arm (17p13). Proc. Natl. Acad. Sci. USA **83:**130–134.
40. **Miller, C., T. Mohandas, D. Wolf, M. Prokocimer, V. Rotter, and P. H. Koeffler.** 1986. Human p53 localized to short arm of chromosome 17. Nature (London) **319:**783–784.
41. **Nahreini, P., and A. Srivastava.** 1989. Rescue and replication of the adeno-associated virus 2 genome in mortal and immortal human cells. Intervirology **30:**74–85.
42. **Ostrove, J. M., D. H. Duckworth, and K. I. Berns.** 1981. Inhibition of adenovirus-transformed cell oncogenicity by adeno-associated virus. Virology **113:**521–533.
43. **Pinkel, D., J. Landegent, C. Collins, J. Fuscoe, R. Segraves, J. Lucas, and J. Gray.** 1988. Fluorescence in situ hybridization with human chromosome-specific libraries: detection of trisomy 21 and translocations of chromosome 4. Proc. Natl. Acad. Sci. USA **85:**9138–9142.
44. **Rigby, P. W., C. Rhodes, and P. Berg.** 1977. Labelling desoxyribonucleic acid to high specific activity in vitro by nick translation with DNA polymerase I. J. Mol. Biol. **113:**237–252.
45. **Rommelaere, J., and J. J. Cornelis.** 1991. Antineoplastic activity of parvoviruses. J. Virol. Methods **33:**233–251.
46. **Rommelaere, J., and P. Tattersall.** 1990. Oncosuppression by parvoviruses, p. 41–57. *In* P. Tijssen (ed.), Handbook of parvoviruses, vol. II. CRC Press Inc., Boca Raton, Fla.
47. **Salomé, N., B. van Hille, M. Geuskens, and J. Rommelaere.** 1989. Partial reversion of conditional transformation correlates with a decrease in the sensitivity of rat cells to killing by the parvovirus minute virus of mice but not in their capacity for virus production: effect of a temperature-sensitive v-*src* oncogene. J. Virol. **63:**4797–4807.
48. **Sambrook, J., E. F. Fritsch, and T. Maniatis.** 1989. Molecular cloning: a laboratory manual, 2nd ed. Cold Spring Harbor Laboratory, Cold Spring Harbor, N.Y.
49. **Samulski, R. J., L. S. Chang, and T. Shenk.** 1989. Helper-free stocks of recombinant adeno-associated viruses: normal integration does not require viral gene expression. J. Virol. **63:**3822–3828.
50. **Samulski, R. J., A. Srivastava, K. I. Berns, and N. Muzyczka.** 1983. Rescue of adeno-associated virus from recombinant plasmids: gene correction with the terminal repeats of AAV. Cell **33:**135–143.
51. **Samulski, R. J., X. Zhu, X. Xiao, J. D. Brook, D. E. Housman, N. Epstein, and L. A. Hunter.** 1991. Targeted integration of adeno-associated virus (AAV) into human chromosome 19. EMBO J. **10:**3941–3950.
52. **Schlehofer, J. R., M. Ehrbar, and H. zur Hausen.** 1986. Vaccinia virus, herpes simplex virus and carcinogens induce DNA amplification in a human cell line and support replication of a helper virus dependent parvovirus. Virology **152:**110–117.
53. **Schlehofer, J. R., and R. Heilbronn.** 1990. Infection with adeno-associated virus type 5 inhibits mutagenicity of herpes simplex virus type 1 or 4-nitroquinoline-1-oxide. Mutat. Res. **244:**317–320.
54. **Schlehofer, J. R., R. Heilbronn, B. Georg-Fries, and H. zur Hausen.** 1983. Inhibition of initiator-induced SV40 gene amplification in SV40-transformed Chinese hamster cells by infection with a defective parvovirus. Int. J. Cancer **32:**591–595.
55. **Schmitt, J., J. R. Schlehofer, K. Mergener, L. Gissmann, and H. zur Hausen.** 1989. Amplification of bovine papillomavirus DNA by *N*-methyl-*N'*-nitro-*N'*-nitrosoguanidine, ultraviolet irradiation or infection with herpes simplex virus. Virology **171:**73–81.
56. **Southern, E. M.** 1975. Detection of specific sequences among DNA fragments separated by gel electrophoresis. J. Mol. Biol. **98:**503–517.
57. **Sprecher-Goldberger, S., L. Thiry, N. Lefèbvre, D. Dekegel, and F. de Halleux.** 1971. Complement-fixation antibodies to adenovirus-associated viruses, adenoviruses, cytomegaloviruses and herpes simplex viruses in patients with tumors and in control individuals. Am. J. Epidemiol. **94:**351–358.
58. **von Knebel, M., T. Bauknecht, D. Bartsch, and H. zur Hausen.** 1991. Influence of chromosomal integration on glucocorticoid-regulated transcription of growth-stimulating papillomavirus genes E6 and E7 in cervical carcinoma cells. Proc. Natl. Acad. Sci. USA **88:**1411–1415.
59. **Wang, H., and S. Federoff.** 1972. Banding in human chromosomes treated with trypsin. Nature (London) **235:**52–54.
60. **Winocour, E., M. F. Callaham, and E. Huberman.** 1988. Perturbation of the cell cycle of adeno-associated virus. Virology **167:**393–399.
61. **Winocour, E., and I. Keshet.** 1980. Indiscriminate recombination in simian virus 40-infected monkey cells. Proc. Natl. Acad. Sci. USA **77:**4861–4865.
62. **Yalkinoglu, A. Ö., J. R. Schlehofer, and H. zur Hausen.** 1990. Inhibition of *N*-methyl-*N'*-nitro-*N*-nitrosoguanidine-induced methotrexate and Adriamycin resistance in CHO cells by adeno-associated virus type 2. Int. J. Cancer **45:**1195–1203.
63. **Yalkinoglu, A. Ö., H. Zentgraf, and U. Hübscher.** 1991. Origin of adeno-associated virus DNA replication is a target of carcinogen-inducible DNA amplification. J. Virol. **65:**3175–3184.